HEFAT2012
9th International Conference on Heat Transfer, Fluid Mechanics and Thermodynamics
16 – 18 July 2012
Malta

EXPERIMENTAL STUDY FOR LOCAL AIR/WATER FLOW STRUCTURE OF BUBBLY AND SLUG FLOW REGIME

D.J. Euh[1*], V.T.Nguyen[1], B.J.Yun[2], C.-H.Song[1]
*Author for correspondence
[1]Korea Atomic Energy Research Institute, P.O.Box 105, Yuseong, Daejeon, 305-600, Rep. of KOREA,
E-mail: djeuh@kaeri.re.kr

[2]Pusan National Univ., Pusandaehakro-63, Geumjeongu, Busan, 609-735, Rep. of KOREA,

ABSTRACT

A study for local hydraulic characteristics of water and air/steam mixture flow is a very challenging topic for advanced thermal hydraulic analysis code development. Recently, many researchers made efforts in the study of mechanistic feature related to the two phase dynamics such as an interfacial area transport model. The mechanistic study for the interfacial area needs a lot of understanding for the bubble/drop dynamics and flow propagation phenomena. To generate an experimental data base for a modeling, an air/water test was performed in this study. The facility has a cylindrical acryl test section of which the diameter and height are 80 mm and 10m, respectively. The major local parameters to be measured are the void fraction, bubble/liquid velocities, interfacial area concentration and bubble size. To investigate the transport phenomena of the two-phase parameters, a local probe and an impedance void meter(IVM) are installed at three axial elevations of the test section. (L/D=12.2, 42.2, 100.7) The test range covers 0.5~2.8 m/s and 0.04~1.2 m/s of the superficial liquid and gas velocity, respectively, which corresponds to the bubbly and slug flow regimes. The system pressure conditions are 0.2~0.3 MPa at the L/D=12.2.

INTRODUCTION

A flow regime map has been utilized for the models related to the energy and momentum transfer of a two-phase flow. Since most of the models are not based on the fundamental phenomenological mechanisms, they sometimes have limitations for application to the general flow conditions. As a new approach, mechanistic studies for the interfacial area transport are being performed to reduce or eliminate the dependency on the flow regime map. The mechanistic study needs a lot of understanding for the bubble/drop dynamics and flow propagation phenomena. The major interaction on bubbles can be characterized by coalescence and breakup in an adiabatic condition. The coalescence of bubbles is induced by random collision, wake entrainment or laminar shear. The breakup of a bubble is induced by collision with turbulent eddy, shearing off or hydraulic instability. [1-2] The accuracy of the interfacial area transport model strongly depends on the appropriateness of the bubble/drop interaction models, which should be developed based on a lot of phenomenological investigations.

To investigate the fundamental two-phase flow phenomena and to generate an experimental data base for a modeling, an air/water test is performed in this study. The test facility has a cylindrical acryl test section of which the diameter and height are 80 mm and 10m, respectively. The local two-phase parameters were measured by five-sensor conductivity probes and bi-directional flow tubes. To investigate the transport phenomena of the two-phase parameters, the local probe and an impedance void meter (IVM) are installed at three axial elevations of the test section (L/D=12.2, 42.2, and 100.7). The test range covers 0.5~2.8 m/s and 0.04~1.2 m/s of the superficial liquid and gas velocity, respectively, which corresponds to the bubbly and slug flow regimes.

TEST FACILITIES

Figure 1 shows a brief configuration of the air/water test facility. The facility has a cylindrical acryl test section of which the diameter and height are 80 mm and 10m, respectively. The local bubble parameters are measured by five-sensor conductivity probes, which are the void fraction, bubble velocity, bubble frequency, interfacial area concentration and bubble size. For a local liquid velocity, a bi-directional flow tube was utilized. The local probes and impedance void meter were installed at axially three positions to investigate the transport phenomena of the two-phase parameters. The system temperature was measured by RTD at the inlet of the test section, which is controlled by means of a pre-heater in the upstream of the test section and a cooler in the storage tank. The pressures at the three elevations, where the conductivity probes are installed, were measured by using the ROSEMOUNT transmitters, of which the error is 0.075% of

the applied measuring span. The pressure at the first elevation is measured by a pressure transmitter. The pressures at the second and third elevations are measured by two differential pressure transmitters. The operating condition is controlled to 0.2 MPa or 0.3MPa and 30°C at the elevation where the first probe is installed. The flow rates of the water and air were measured by using Micromotion Coriolis flow meter, of which the error is 0.2% and 0.5%, respectively.

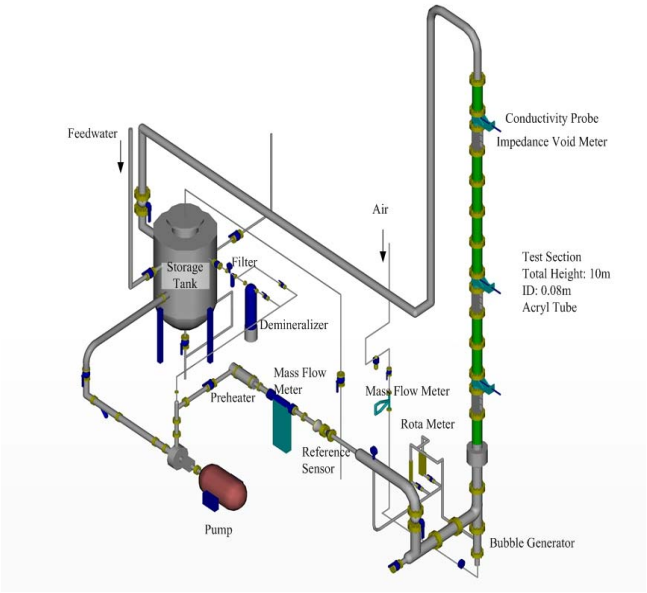

Figure 1 A bird-eye view of test loop

The various bubble parameters are measured by using conductivity probes. The conductivity probe method uses the principle of phase discrimination by using the electrical conductivity difference between the water and gas phases. Figure 2 shows the design of the conductivity probe used in this study. The probe is inserted from the side of the test section and moved to the given point by a traversing system. The conductivity probe includes five sensors in a probe, which consists of a sensing part, sensor supporter, probe body, connector, and enamel wires, and so on, as shown in figure 2. The thickness of the bare needle is 0.18mm and the final coated sensor thickness is 0.25mm. The lateral length between the symmetrical rear sensor tips is 1.0mm and the vertical distance between the central front and rear sensor tips is 2.0mm. Central rear sensor is 0.25mm apart from the centerline.

The five-sensor conductivity probe is designed to efficiently measure the interfacial area concentration of bubbles having various shapes and motions. [3-5] The void fraction and bubble frequency can be measured by using only the front sensor. The bubble velocity and bubble chord length are measured by using the front and rear sensors. The bubble size can be obtained from the measured void fraction and the interfacial area concentration by the following formula.

$$D_{Sm} = \frac{6\alpha}{a_i}$$

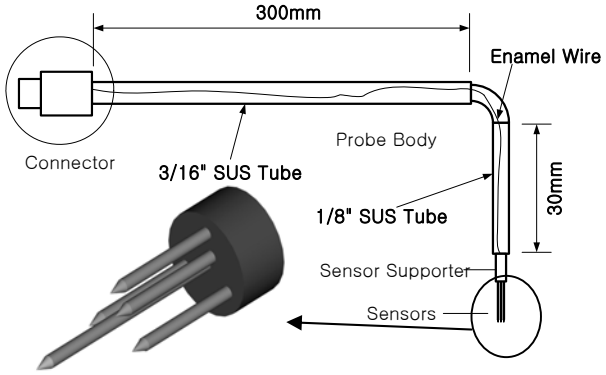

Figrue 2 Five-Sensor Probe

External AC current is activated to the probe and the conductivity information of the two-phase mixture at the sensor tips is conveyed to the signal conditioner. The signal conditioner rectifies the AC currents and eliminates the high frequency components due to the noise by a low pass filter. The signals are then delivered to the terminal boards. Finally, the analog signals are converted to the digital signals with the A/D converter included in the IBM PC. At first, the digitized raw signals should be converted to a rectangular form. This process means an explicit definition of the phase. The following step is to find the same bubble signal in the two sensor signals. After finishing the above procedures, we can obtain various physical parameters such as the void fraction, velocity, interfacial area concentration, bubble frequency, bubble diameter, and so on. We used HP-VEE for the overall processing environment. The key process is performed by an external user function that is built with Visual C++.

RESULTS

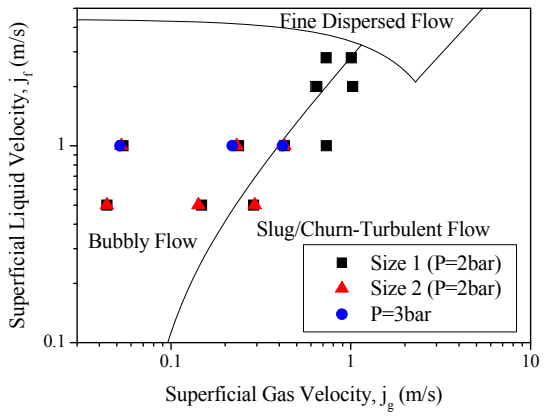

Figure 3 Test conditions on Flow Regime Map

The test matrix covers the bubbly and slug flow regime as shown in figure 3. The Titel and Dukler's flow regime map was cited in this study.[6] The test cases consist of three categories: (1) 11 base cases (2) 6 Small Bubble cases (3) 3 Elevated pressure conditions. The test range covers 0.5~2.8 m/s and

0.04~1.01 m/s of the superficial liquid and gas velocity, respectively, which corresponds to the bubbly and slug flow regimes. The system pressure conditions are 0.2~0.3 MPa at the L/D=12.2. Various transport data of local two-phase parameters can be obtained. In order to investigate the data consistency, the area averaged data of local parameters were compared with global measured parameters. The void fraction from the conductance probe was compared with the impedance void meter data, which agreed well within 9.1% of deviation. At higher void fraction conditions, the probe data slightly underestimate the data from the impedance void meter. A complicated signal shape induced by bubble clusters can be considered as one of the reasons of deviation for the high void fraction conditions. Air velocity and superficial velocity by using conductance probe were agreed well withing 10% and 11.8%, respectively those from the flow meter and impedance void meter. The liquid velocity and superficial velocity have 7.3% and 7.5% of discrepancy between local and global parameters. The underestimation of the liquid velocity at higher velocity conditions is mainly due to the deviation of the void fraction measured by the conductance probe while the mass flow rate is converted to liquid velocity.

The results of comparison were shown in figures 4 to 8.

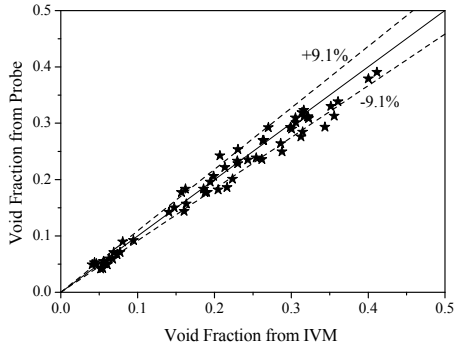

Figure 4 Comparison of Void Fraction

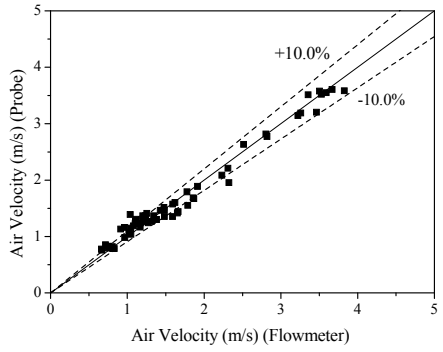

Figure 5 Comparison of Air Velocity

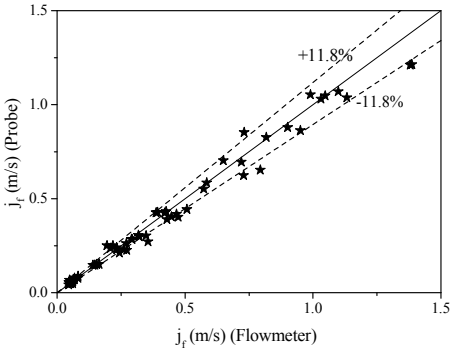

Figure 6 Comparison of Superficial Air Velocity

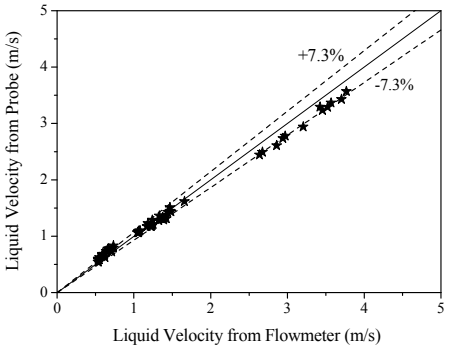

Figure 7 Comparison of Liqiud Velocity

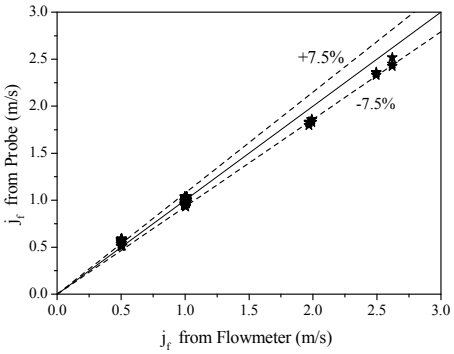

Figure 8 Comparison of Superficial Liquid Velocity

The transport phenomena of various channel averaged two-phase parameters, such as the pressure, void fraction can be analyzed from the experimental data. Figure 9 shows the variation of the pressure along the test section. As the flow goes upward, the pressure is decreased due to a hydrostatic head reduction. For the fixed liquid flow condition, the pressure reduction becomes smaller for the high void fraction cases than that for the low void fraction cases. The void fraction at the upper position of the test section is larger than that at the lower

level since the air density becomes smaller due to the pressure reduction. Figure 10 shows the trend well.

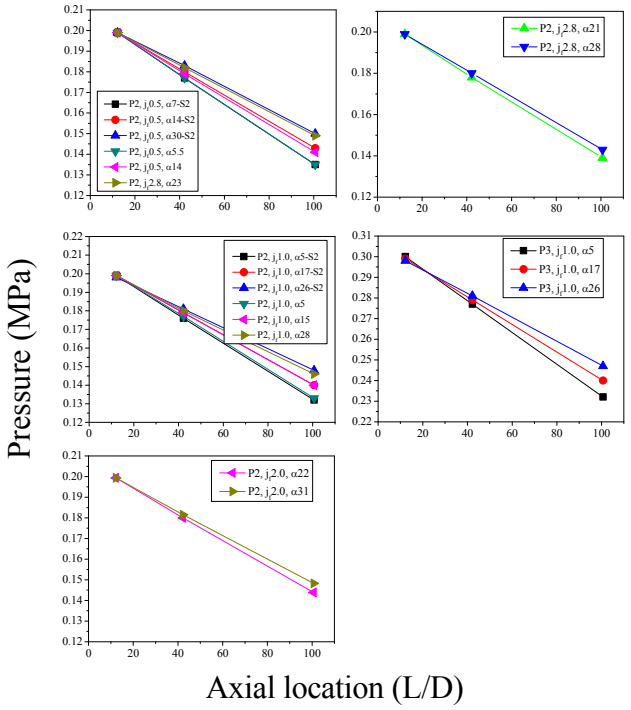

Figure 9 Transport of pressure

Figure 11 shows the transport phenomena of local profile of two-phase mixture for the typical bubbly flow conditions. A significant wall peaking feature was shown in this flow condition. The local profile of the void fraction depends on the lift force which depends on the bubble size and velocity. The experimental results show that the degree of wall peaking becomes more remarkable as the mixture flows upward. The velocity profile of local bubbles and liquid has a central peak distribution due to the effect of wall friction. The air velocities are slightly increased along with the increasing void fraction as flow goes upward as shown in figure 11.

Figures 12~14 show a results for the two phase transport phenomena for slug flow conditions. The cap/slug flow structure consists of small bubble and cap/slug bubbles, which was defined as 1st and 2nd group in the figures 12 to 14. As cap/slug bubbles form, the interfacial structure varies remarkably when compared with small size of bubbly flow conditions. As two-phase flow goes upward, the overall void fraction is increased due to the volumetric expansion by reduced hydrostatic head effect. The void fraction of the second group bubbles is increased as shown in figure 12. In the mean while the void fraction of small bubbles slightly reduced. From the trend of the flow characteristic, wake entrainment mechanism can be analogized to be important for the flow conditions. Figure 13 showes a transport of local bubble size. The first bubble group size does not vary significantly; in the mean while, cap/slug bubble size is increased remarkably, which also reflects active wake entrainment induced coalescence mechanism. The local void fraction and air/liquid velocities show a classical central peaking. Along with the increasing void fraction as the flow goes upward, the increasing trend is well shown in the bubble and liquid velocity profiles of figure 14.

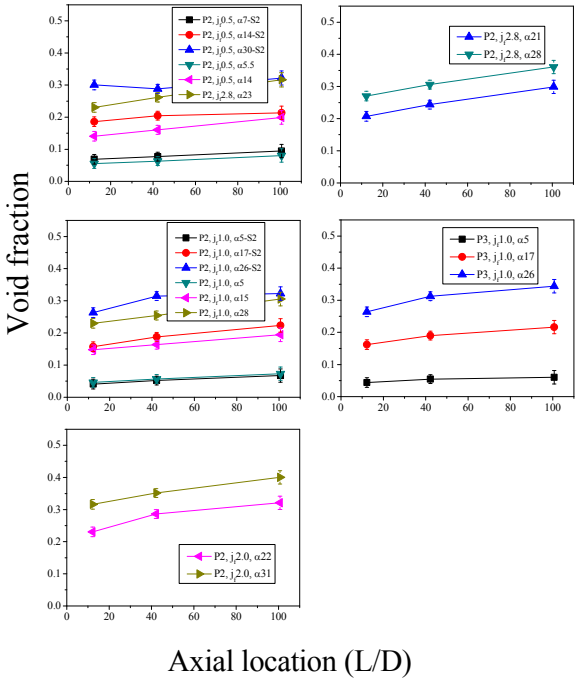

Figure 10 Transport of Void Fraction

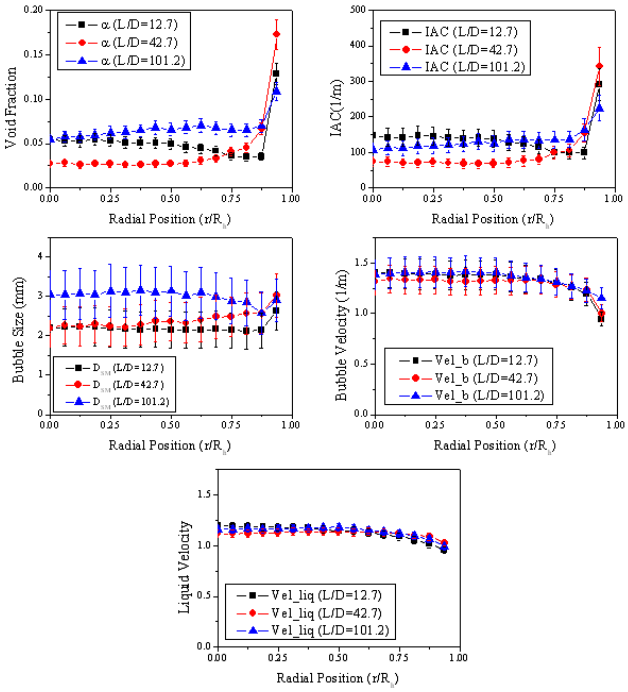

Figure 11 Transport of local parameters for bubbly flow conditions ($<j_f>$=1.0, $<j_g>$=0.054. $<\alpha>_{1st}$=5.1%)

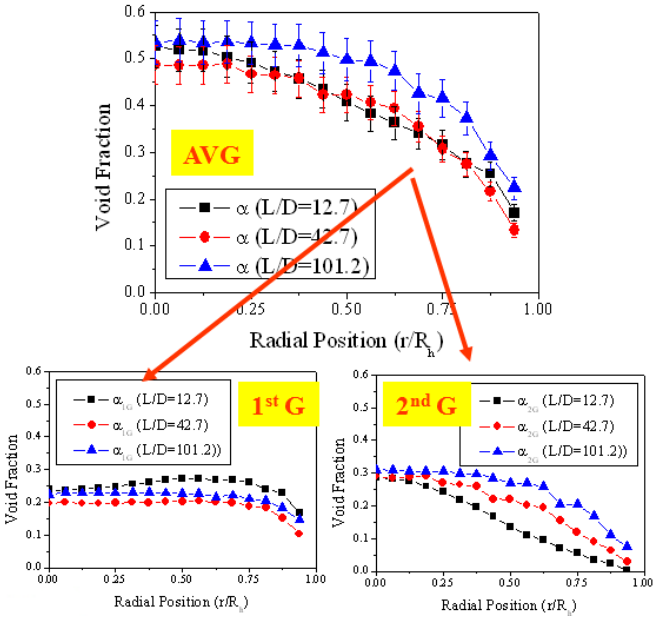

Figure 12 Transport of local void fraction of slug flow condition ($\langle j_f \rangle$=1.0, $\langle j_g \rangle$=0.73. $\langle \alpha \rangle_{1st}$=31.5%)

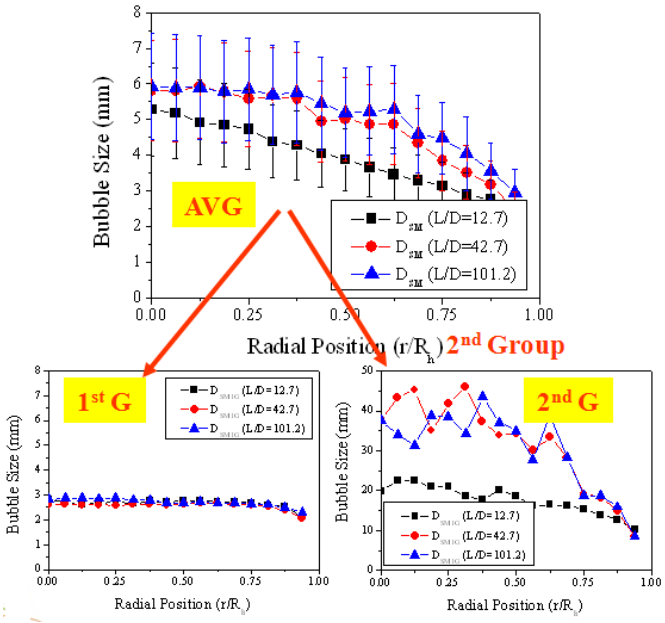

Figure 13 Transport of local bubble size of slug flow condition ($\langle j_f \rangle$=1.0, $\langle j_g \rangle$=0.73. $\langle \alpha \rangle_{1st}$=31.5%)

Figure 15 shows a transport of bubble chord length distribution for various flow conditions. Although the distribution is not for a bubble diameter but for a chord length, the transport characteristics of chord length distribution can approximate those of the bubble size distribution. The figure shows the variation of the bubble size spectrum as a two-phase mixture flows upward. The transport phenomena can be explained by a mechanism related to the interaction between bubbles and/or a bubble and local turbulence structure. At a higher elevation, the number of large bubbles is increased; in the meanwhile, the number of small bubbles is decreased. From the shift of bubble size spectrum, wake entrainment can be considered as an important mechanism for the transport of two-phase mixture for this flow condition.

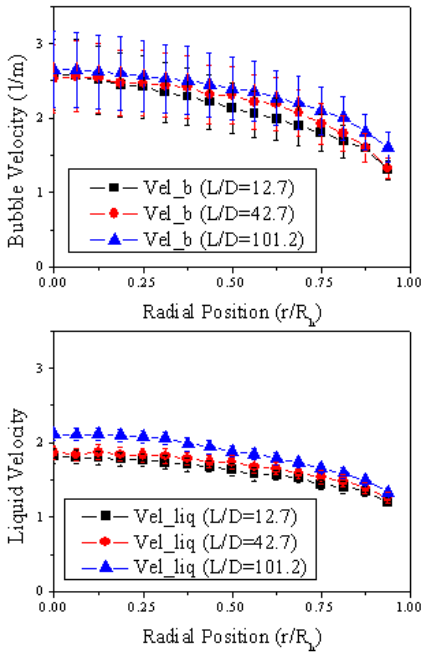

Figure 14 Transport of local velocities of slug flow condition (Run16; $\langle j_f \rangle$=1.0, $\langle j_g \rangle$=0.73. $\langle \alpha \rangle_{1st}$=31.5%)

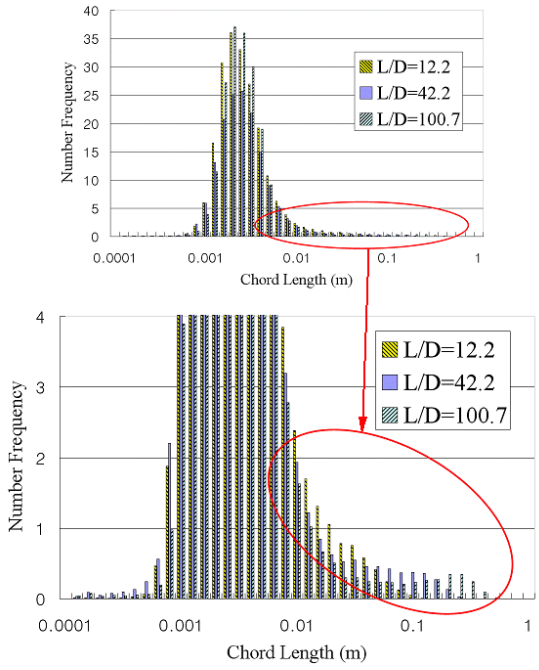

Figure 15 Transport of Bubble Size Distribution ($\langle j_f \rangle$=1.0, $\langle j_g \rangle$=0.73. $\langle \alpha \rangle_{1st}$=31.5%)

CONCLUSION

To investigate the transport phenomena of two-phase flow, air/waters tests were performed. Various local bubble parameters and liquid velocity were measured for the bubbly and slug flow regime conditions. From the data of the various two-phase bubble parameters, the mechanisms which affect variation of the two-phase flow structure can be analyzed. The data produced in this study will be effectively utilized for the development of the interfacial area transport model.

ACKNOWLEDGEMENT

This work has been financially supported by the Ministry of Education, Science and Technology (MEST) of Korean government under the national nuclear mid- & long-term R&D program

NOMENCLATURE

$\langle\rangle$	area average
D	Hydraulic Diameter
D_{Sm}	Bubble Sauter Mean Diameter
α	Void Fraction
a_i	Interfacial Area Concentration
j_f	Superficial Liquid Velocity
j_g	Superficial Gas Velocity
L	Pipe Length

REFERENCES

[1] Prince M. J. and Blanch H. W., "Bubble Coalescence and Break-up in Air-Sparged Bubble Columns, AIChE, vol. 36, No. 10 (1990)

[2] T. Hibiki and M. Ishii, "Two-Group Interfacial Area Transport Equations at Bubbly-to-Slug Flow Transition", Nuclear Engineering and Design, Vol. 202, pp. 39-76 (2000)

[3] D.J. Euh, A Study on the Measurement Method and Mechanistic Prediction Model for the Interfacial Area Concentration, Ph. D Thesis, Seoul Univ. (2002)

[4] D.J. Euh, B.J. Yun, B.G. Huh, W.M. Park, C.-H. Song, C.H. Chung, "Signal Processing Scheme and Evaluation for Five-Sensor Probe Method", KNS Meeting (2004)

[5] D.J. Euh, B.J. Yun, C.H. Song, "Numerical Simulation of an improved five-sensor probe method for local interfacial area concentration measurement", to be published, Nucl. Eng. and Design (2004)

[6] Y. Taitel, D.Bornea, and A.E. Dukler, "Modeling Flow Pattern Transitions for Steady Upward Gas-Liquid Flow in Vertical Tubes, AIChE, Vol. 26, No. 3 pp. 345 354 (1980)